

The Effect of Shear Flow on the Helfrich Interaction in Lyotropic Lamellar Systems

Simon W. Marlow and Peter D. Olmsted

e-mail: physwm@irc.leeds.ac.uk and p.d.olmsted@leeds.ac.uk

Polymer IRC and Department of Physics & Astronomy, University of Leeds, Leeds LS2 9JT, UK

Received: October 28, 2018/ Revised version: date

Abstract. We study the effect of shear flow on the entropic Helfrich interaction in lyotropic surfactant smectic fluids. Arguing that flow induces an effective anisotropic surface tension in bilayers due to a combination of intermonolayer friction, bilayer collisions and convection, we calculate the reduction in fluctuations and hence the renormalised change in effective compression modulus and steady-state layer spacing. We demonstrate that non-permeable or slowly permeating membranes can be susceptible to a undulatory instability of the Helfrich-Hurault type, and speculate that such an instability could be one source of a transition to multilamellar vesicles.

PACS. 64.70.Md Transitions in liquid crystals – 83.80.Qr Rheology of surfactant and micellar systems, associated polymers – 87.16.Dg Membranes, bilayers, and vesicles

1 Introduction and Overview

Lamellar systems display a wide variety of behaviours in the presence of shear flow. Weak flows typically align lamellae so that they slide over one another with layer normals parallel to the flow-gradient ($\nabla \mathbf{v}$) direction (c orientation in Fig. 1.1). Lamellar block-copolymer melts undergo a series of reorientation transitions as a function of strain rate, frequency, and amplitude, between the c and a (layer normals parallel to the vorticity (ω) direction) orientations [1,2,3,4]. Thermotropic smectic liquid crystals also undergo a variety of reorientational transitions as a function of strain rate [5,6]. Lyotropic smectics, such as surfactant lamellar systems, can form multi-lamellar vesicles, or “onions”, either above a critical strain rate (see [7,8,9] for studies of SDS surfactant systems), or for very small (essentially zero) strain rates (see [10] and [11] for studies of AOT and ionic systems, respectively). At higher strain rates these onions can undergo further transitions to onion crystals of different symmetries and sizes [12,13] as well as to oscillatory states [14]. Scattering experiments on some lyotropic and thermotropic smectics (main chain and side chain) suggest other multilamellar curved structures, such as concentric cylinders, or “leeks” [15,16,17]. Onion formation and layer rearrangement have been correlated with screw dislocations in DMPC/ $C_{12}E_5$ solutions [18]. Onions have also been seen in triblock copolymer solutions [19].

The relative and absolute stability of the a and c orientations has been understood from several points of view, but there is no clear picture yet that indicates which mechanisms operate in which systems. Cates and Milner pre-

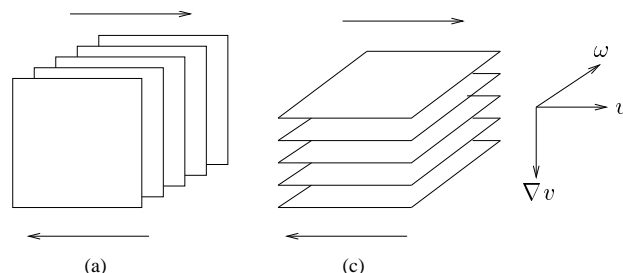


Fig. 1.1. Orientations of a Lamellar Phase in Shear Flow

dicted that shear can stabilise a layered system near the equilibrium sponge-lamellar phase transition [21]; such a transition has been reported experimentally [22,23]. Ramaswamy [24] argued that shear flow can suppress undulations in the a orientation, leading to a collapse of the lamellar phase. The dependence of the critical shear rate, $\dot{\gamma}_c$ on layer spacing, d and membrane viscosity η was calculated to be $\dot{\gamma}_c \sim (k_B T)^3 / \eta \kappa^2 d^3$. Such a collapse was seen in the flow of a thin lamellar phase of the ionic surfactant AOT in brine, in a specially designed Couette cell assumed to shear the layers in the a orientation [25]. The dependence on layer spacing matched Ramaswamy’s prediction, if the measured d -dependence of the zero shear viscosity ($\eta \sim 1/d^2$) was incorporated. However, viscosity measurements were performed in a standard Couette cell rheometer; there is some evidence that AOT orders in the c -orientation in such a geometry [26]. In addition a

slightly different dependence of the critical shear rate on layer spacing was found for a lamellar phase consisting of an anionic surfactant, a deviation that might be explained by the presence of the more dominant Helfrich interaction. To further understand these experiments, in addition to disentangling the viscosity issues, it may be important to consider the propagation of the air/fluid interfacial surface tension into the bulk.

Milner and Goulian [27] examined the instability of thermotropic smectics in the c orientation, and noted that convection of bending fluctuations can induce compression and destabilises the c orientation with respect to the a orientation. Fredrickson showed that non-linearities in the diblock free energy can destabilise the c orientation with respect to the a orientation [2]. Another mechanism is viscous contrast [28, 4]: the c phase allows the strain field to be concentrated in the less viscous material, which would be favoured at higher frequencies or strain rates.

Although the appearance of the onion phase in shear flow is well-documented, there is still no reliable theoretical framework for this phenomenon. An appealing device for the onion instability is an analogy of the Helfrich-Hurault mechanism [29, 30], in which an applied dilational strain parallel to the layer normals may be relieved by buckling to retain the equilibrium layer spacing. Oswald and Kleman [31] proposed that a smectic flowing between misaligned plates generates defects that induce the necessary dilational strain, and Roux and co-workers used this argument to rationalise their results [7]. The shear rate $\dot{\gamma}_c$ for buckling was estimated to vary inversely with the square of the gap size between the plates. However, not only do experiments show that the gap size does not affect $\dot{\gamma}_c$ [16], but the predicted value for $\dot{\gamma}_c$ differs from the observed value by a few orders of magnitude. Wunenburger and co-workers [32] extended this idea to consider the higher shear-rate transition from onions to another well-oriented lamellar phase. They demonstrated that, at high enough strain rates, an undulation could persist in the velocity gradient direction while a restabilisation would occur in the velocity direction. Reasonable comparisons were made between the resulting theoretical stability diagrams and the experimentally observed transitions.

In the case of thermotropic smectics, Auernhammer and co-workers [33] suggested that flow can induce a layer tilt due to brushing of molecules in adjacent layers aligned parallel to the normal. This induces an effective strain due to the layer shrinkage in the normal direction (if there are few defects and the necessary change in layer number cannot occur) that can, in principle, be large enough to destabilise the c orientation. Unpublished simulations [34] found undulations in the vorticity direction.

In this work we consider the entropic, collision dominated membranes first studied by Helfrich [35], and neglect the effect of electrostatic forces. Shear flow has a dramatic effect on the fluctuation spectrum, and a reasonable proposition is that flow suppresses fluctuations in the c orientation, hence reducing intermembrane interactions and repulsion between the layers. For systems with many defects, this reduced repulsion would be expected

to lead, after an appropriate time, to a reduction in mean layer spacing. Indeed not only was this seen by Yamamoto and Tanaka [36], but also the shape of the x-ray scattering Bragg peak became broader and less intense. For systems with few defects or very slow permeation, the reduced fluctuation spectrum would lead to an effective imposed strain along the layer normals, which if sufficiently large could be relieved by buckling. This, then, could be a mechanism leading to onion formation, in the event that other considerations allow for onions. For example, the Gaussian curvature modulus $\bar{\kappa}$ should not be too positive, which would tend to suppress structures with positive mean curvature, and the a orientation should also be dynamically unstable.

Our task, then, is to calculate the suppression of layer undulations in the c orientation, and hence the renormalised “interlayer potential” in steady state shear flow. In lieu of potentials, the proper starting point is the full dynamics of a lyotropic smectic [37] in the presence of an imposed boundary stress or strain rate. Rather than taking this approach, we assume a coarse-grained free energy, following Bruinsma and Rabin [40], as a first step towards understanding the effect of flow. In common with the recent work of Zilman and Granek [41], we assume that bilayers oriented in the c orientation experience a flow-induced effective tension, although the tension that we propose is anisotropic and has a different sign and physical interpretation (Appendix A). In Section 2 we explore the effects of this tension on the steady-state layer spacing d and the compression modulus \bar{B} of an equilibrium Helfrich stabilised lamellar phase. In Section 3 we examine these results in the context of an imposed shear flow. After estimating possible sources of tension we discuss the predicted change in layer spacing and the possibility for an instability, taking into account permeation and defect-creation. We finish with a summary in Section 4 and outline future work that will quantitatively address the dynamic origin and consequences of this tension.

There have been several discussions of the effect of flow on the layer spacing in block copolymer lamellar systems, which focus on the change in polymer conformations due to the stretching imposed by flow in melts and solutions [42], and layer changes have been reported in melts [45]. Our mechanism is unrelated to this one, but may be related to recent experiments on block copolymer solutions that have demonstrated a change in layer spacing [46] and onion formation as a function of flow [19], if those systems are Helfrich stabilised.

2 The Lamellar Phase under Tension

2.1 The Equilibrium zero-tension Lamellar Phase

The equilibrium free energy F of a three-dimensional lyotropic smectic fluctuating at fixed chemical potential penalises gradients in the mean layer displacement $u(\mathbf{r})$:

$$F = \frac{1}{2} \int d^3r [K(\nabla_{\perp}^2 u)^2 + \bar{B}(\partial_z u)^2]. \quad (2.1)$$

The elastic constants in Eq. (2.1) are the bending modulus K and the compression modulus at fixed chemical potential \bar{B} . For membranes that interact via collisions the origin of \bar{B} is the steric repulsive interaction [35]; the collisions induce an entropic confinement pressure p ,

$$p \sim \frac{k_B T}{L_p^2 d}, \quad (2.2)$$

where L_p is the characteristic distance between collisions (the “patch” or “collision” length) and d is the layer spacing, from which the compression modulus may be estimated by $\bar{B} \sim -d\partial p/\partial d$

The patch length is the implicit lower cut-off of the integral in Eq. (2.1) and is that transverse distance over which membranes wander before colliding, found by computing the mean fluctuations of a free membrane, governed by the single membrane free energy f . In the Monge gauge,

$$f = \frac{1}{2}\kappa \int_{A_\perp} d^2 r (\nabla_\perp^2 h(\mathbf{r}))^2 = \frac{1}{2}\kappa L^2 \sum_{\mathbf{q}_\perp} |h_{\mathbf{q}_\perp}|^2 q_\perp^4, \quad (2.3)$$

where $h(x, y) = h(\mathbf{r})$ is local height of a given membrane, rather than the mean position $u(\mathbf{r})$ that we introduced above for the coarse-grained three-dimensional free energy. A_\perp is the projected membrane area orthogonal to the mean membrane normal. L is the system size and we have defined the Fourier Transform $h(\mathbf{r}) = \sum_{\mathbf{q}_\perp} h_{\mathbf{q}_\perp} e^{i\mathbf{q}_\perp \cdot \mathbf{r}}$. Assuming periodic boundary conditions,

$$\sum_{\mathbf{q}_\perp} = \left(\frac{L}{2\pi}\right)^2 \int_{\pi/L_p}^{\pi/a} d^2 \mathbf{q}_\perp, \quad (2.4)$$

where a is a molecular size and wavelengths longer than L_p are suppressed by steric hindrance with neighbouring membranes. Note that

$$u(x, y, z = nd) = \int_{A(L_p)} [h(x' - x, y' - y) - nd] \frac{d^2 r'}{A(L_p)} \quad (2.5)$$

is the average of the microscopic layer displacement over a patch area $A(L_p)$ centred at $(x, y, z = nd)$, so that Eq. (2.1) encompasses Eq. (2.3) subject to a hard wall constraint and $K = \kappa/d$.

We neglect the Gaussian curvature, penalised by the modulus $\bar{\kappa}$, which is valid for fixed topology. However, transitions to a different topology such as onions, or changes in the distribution of dislocations or pores [47], may involve $\bar{\kappa}$. Quantities known to alter $\bar{\kappa}$, such as salinity, temperature, or cosurfactant, seem to influence the shear rate and/or the mechanism for onion formation [10, 48, 49, 50].

The compression modulus may be estimated by relating L_p to d [35]. The constraints of neighbouring membranes limits the mean square fluctuations to the mean layer spacing d^2 ,

$$\langle h^2(\mathbf{r}) \rangle = \alpha d^2, \quad (2.6)$$

where α is a constant of proportionality. The calculation of the mean square fluctuations is straightforward:

$$\langle h^2(\mathbf{r}) \rangle = \sum_{\mathbf{q}_\perp} \langle |h_{\mathbf{q}_\perp}|^2 \rangle = \frac{k_B T}{4\pi^3 \kappa} L_p^2, \quad (2.7)$$

where $L_p/a \gg 1$. The constraint on the height fluctuations Eq. (2.6) leads to an expression for the collision length,

$$L_p = cd \sqrt{\frac{\kappa}{k_B T}}. \quad (2.8)$$

If $\alpha = 1/3\pi^2$, as inferred by Helfrich [35], then $c = \sqrt{4\pi/3}$. There is some debate about the exact value of c ; for example, Golubovic and Lubensky [51] calculated $c = \sqrt{32/3\pi}$.

Combining the collision length with the pressure (Eq. 2.2) yields a compression modulus that has been calculated precisely as [35, 52, 53]

$$\bar{B} = \frac{6\delta_n n}{n+1} \frac{(k_B T)^2}{\kappa d^3}, \quad (2.9)$$

where n is the number of membranes. For $n = \infty$ Helfrich determined $\delta_\infty = 3\pi^2/128 \sim 0.23$ [35]. Strong coupling perturbation calculations [52] suggest that $\delta_\infty \sim 0.1$ and for a single membrane, $\delta_1 = \pi^2/128 \sim 0.07$; both results are consistent with those given by Monte-Carlo simulations [53].

For flat membranes in a lamellar phase the volume fraction is given by $\phi = t/d$, where t is the layer thickness. For fluctuating lamellar phases of uniform thickness t , the mean volume fraction is

$$\phi = \left\langle \frac{A}{d} \right\rangle \frac{t}{A_\perp}, \quad (2.10)$$

where A is total membrane area. To find the relation between layer spacing and concentration, we can expand (for given mean spacing d) $A \simeq A_\perp (1 + \frac{1}{2} \langle (\nabla_\perp h)^2 \rangle)$, to find

$$d = \frac{t}{\phi} \left[1 + \frac{1}{2} \langle (\nabla_\perp h)^2 \rangle \right] \quad (2.11a)$$

$$= \frac{t}{\phi} \left[1 + \frac{k_B T}{4\pi\kappa} \ln \left(c \frac{d}{a} \sqrt{\frac{\kappa}{k_B T}} \right) \right]. \quad (2.11b)$$

Membranes dominated by electrostatic interactions are essentially flat, in which case $d\phi$ is independent of the volume fraction ϕ . Hence, deviation from this ‘ideal’ dilution law according to Eq. (2.11) suggests that the membranes are stabilised by the Helfrich interaction [54]. Use of Eq. (2.11), given d and t , allows κ and a to be extracted from swelling experiments. Helfrich systems include various dilute non-ionic and screened surfactant solutions. Whether or not certain dilute copolymer solutions that form onions under shear [19] are stabilised by the Helfrich interaction is unclear. Further evidence of Helfrich stabilisation is deduced from the power law behaviour exhibited by the x-ray structure factor [55], from which the bending modulus can be extracted.

2.2 Lamellar Phase subjected to a Finite Anisotropic Tension

2.2.1 Equilibrium Layer Spacing

When a Helfrich-stabilised lamellar phase is sheared in the c orientation, layers are convected and stretched by the flow, adjacent fluctuating layers collide, and flow induces the leaves of the bilayer to slide over one another. A rigorous study of the effect of flow on membranes should consider appropriate equations of motion and treat the dynamics explicitly. For example, the best approach, albeit probably intractable, would be to coarse-grain a dynamical description of coupled monolayers such as that of Ref. [56] to an effective two-component smectic theory, incorporating both flow and the normal and tangential collision forces. We adopt instead a ‘quasi-equilibrium’ approach to gain insight into the stability of the steady states for membranes in flow. We propose that the resulting interplay of hydrodynamic interactions and interbilayer friction can be described by a flow-induced effective tension acting parallel to the layers.

In the presence of a tension, Seifert’s [58] self-consistent calculation of the potential between a wall and a membrane of a vesicle under tension might be applied to find the preferred separation. However, since repulsive interactions from neighbouring membranes dominate the interlamellar potential far from the unbinding transition [59], a similar derivation of the layer spacing cannot be achieved. Thus we are led to deduce a new layer spacing without regard for the change in potential by generalising Helfrich’s geometric argument leading to the dilution law Eq. (2.11) to include a lateral tension [60].

To retain the asymmetry between flow and vorticity directions in the plane, we model the flow as an effective anisotropic tension applied in the flow direction. The free energy of a membrane subject to an anisotropic tension σ is

$$f = \frac{1}{2} \int d^2r \left[\kappa (\nabla_\perp^2 h)^2 + \sigma (\nabla_x h)^2 \right], \quad (2.12)$$

where σ penalises short wavelength modes and the increased area due to stretching the membrane in the x -direction. This decreases the excess area and suppresses fluctuations:

$$\langle h^2(\mathbf{r}) \rangle = \frac{k_B T}{(2\pi)^2} \int_{\pi/L_p}^{\pi/a} \frac{d^2 \mathbf{q}_\perp}{\kappa q_\perp^4 + \sigma q_x^2} \quad (2.13a)$$

$$= \frac{k_B T}{2\pi\sigma} \left(\sqrt{1 + \frac{\sigma L_p^2}{\kappa\pi^2}} - 1 \right), \quad (2.13b)$$

for $L_p/a \gg 1$. Here we assume an isotropic change in patch length, rather than the anisotropic renormalisation that would be expected; this should suffice for qualitative behaviour, as we show below. Assuming the same hard wall constraint as without tension, Eq. (2.6), we can calculate a renormalised mean patch length,

$$L_p^2 = 4\pi^3 \alpha d^2 \frac{\kappa}{k_B T} \left(1 + \alpha \pi \frac{\sigma d^2}{k_B T} \right). \quad (2.14)$$

By the equipartition theorem,

$$\langle (\nabla_\perp h(\mathbf{r}))^2 \rangle = \frac{k_B T}{(2\pi)^2} \int_{\pi/L_p}^{\pi/a} \frac{q_\perp^2 d^2 \mathbf{q}_\perp}{\kappa q_\perp^4 + \sigma q_x^2} \quad (2.15a)$$

$$= \frac{k_B T}{2\pi\kappa} \left[\ln \frac{L_p}{a} - \ln \left| \frac{1 + \sqrt{1 + \frac{\sigma L_p^2}{\kappa\pi^2}}}{1 + \sqrt{1 + \frac{\sigma a^2}{\kappa\pi^2}}} \right| \right]. \quad (2.15b)$$

The simultaneous conditions relating the patch size to the layer spacing via $\langle h^2 \rangle$ (Eq. 2.13a), and the concentration to the degree of crumpling $\langle (\nabla_\perp h)^2 \rangle$ (Eq. 2.11a) determine the layer spacing as a function of concentration and tension, $d(\phi, \sigma)$, as well as the associated collision length $L_p(\phi, \sigma)$. Hence, using Eq. (2.14) to eliminate L_p^* , we find

$$\hat{d} = \hat{d}_0 + \frac{1}{4\pi k} \ln \left| \frac{\hat{d}}{\hat{d}_0} \left(\frac{1 + \sqrt{1 + \frac{\hat{\sigma}}{\hat{d}_0^2} \frac{1}{k} \left(\frac{\phi}{ct} \right)^2}}{2\sqrt{1 + \frac{\hat{\sigma}}{4} \left(\frac{\hat{d}}{\hat{d}_0} \right)^2}} \right) \right| \quad (2.16)$$

where $\hat{d} = d\phi/t$, $\hat{t} = t/a$, $k = \kappa/k_B T$ and $\hat{\sigma} = 4\pi\alpha\sigma d_0^2/k_B T$ are non-dimensionalised parameters and d_0 is the layer spacing at zero tension. As expected, an increasing tension reduces the excess area.

For $\hat{\sigma} \ll 1$ we can calculate the change in the preferred layer spacing,

$$d = d_0 \left[1 - \frac{\sigma d_0^2}{k_B T} \left(\frac{\frac{1}{2} - \frac{k_B T}{\kappa} \left(\frac{a}{cd_0} \right)^2}{\frac{4\pi\kappa}{k_B T} \frac{\phi}{t} d_0 - 1} \right) \pi\alpha + \dots \right]. \quad (2.17)$$

Note that the linear correction is half that of a membrane subjected to isotropic tension. The asymptotic expression for high tension is

$$d = \frac{t}{\phi} \left(1 + \frac{k_B T}{4\pi\kappa} \frac{c}{a} \sqrt{\frac{\kappa}{4\pi\alpha\sigma}} \right). \quad (2.18)$$

The relative reduction in layer spacing, calculated from Eq. (2.16), is shown in Fig. 2.1. This applies directly to equilibrium systems with a mechanically-applied tension, such as few-layered vesicles or bilayers tethered to surfaces. Tension should have the greatest effect when acting on the largest excess surface area, and hence we expect a greater decrease in layer spacing for a lower bending modulus and large crumpling fraction.

As mentioned above, we have assumed that the patch length increases isotropically with increasing tension, and hence imposed a cylindrical geometry with a change in the lower radius cutoff π/L_p . Physically, one would expect, at least for small tensions, that the patch size would actually increase anisotropically, with fluctuations in the transverse direction less affected by stretching. In this case

* For an isotropic tension the swelling law is $\hat{d} = \hat{d}_0 + \frac{1}{8\pi k} \left\{ \ln \left[1 + \frac{\hat{\sigma}}{\hat{d}_0^2} \frac{1}{k} \left(\frac{\phi}{ct} \right)^2 \right] - \ln \left[\hat{\sigma} + \hat{\sigma} \left(e^{\hat{\sigma} \hat{d}^2 / \hat{d}_0^2} - 1 \right)^{-1} \right] \right\}$.

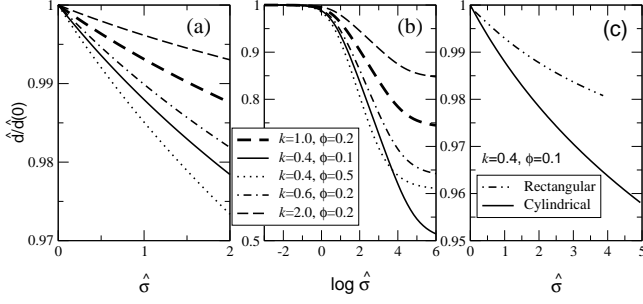


Fig. 2.1. Fractional change in layer spacing \hat{d}/\hat{d}_0 for the isotropic (cylindrical) patch length renormalisation, from Eq. (2.16) and Eq. (2.11) at $\hat{t} = 6$ as a function of induced tension $\hat{\sigma}$ for small values (a) and $\log \hat{\sigma}$ for all values (b). (c) A comparison of cylindrical (Eq. 2.16) and rectangular (Eqs. 2.19) patch size renormalisations, for $k = 0.4$, $\phi = 0.1$. Note $k = \kappa/k_B T$ and $c = \sqrt{4\pi/3}$.

one should impose a rectangular domain of integration, with a cutoff π/L_{py} for the q_y integration, which remains fixed for increasing σ , and a cutoff $\pi/L_p(\phi, \sigma) \leq \pi/L_{py}$ for the q_x integration, which decreases for increasing σ . In this case the simultaneous set of equations that determines the new layer spacing d and patch size L_p is:

$$\alpha d^2 = \frac{k_B T}{4\pi^2} \int_{\pi/L_{py}}^{\pi/a} dq_y \int_{\pi/L_p(\phi, \sigma)}^{\pi/a} dq_x \frac{1}{\kappa(q_x^2 + q_y^2)^2 + \sigma q_x^2} \quad (2.19a)$$

$$\frac{\phi d}{t} = 1 + \frac{k_B T}{8\pi^2} \int_{\pi/L_{py}}^{\pi/a} dq_y \int_{\pi/L_p(\phi, \sigma)}^{\pi/a} dq_x \frac{(q_x^2 + q_y^2)}{\kappa(q_x^2 + q_y^2)^2 + \sigma q_x^2} \quad (2.19b)$$

Results of this calculation for a representative parameter set are shown in Fig. 2.1c. As expected, the inclusion of an anisotropic patch size leads to a smaller layer spacing shrinkage, because the transverse fluctuations remain substantial. Note, however, that solutions do not exist above for $\hat{\sigma} \simeq 4.0$. Formally, this limit corresponds to $L_p \rightarrow \infty$ with L_y finite, and describes layers that are essentially flat in the tension direction while crumpled in the transverse direction. Microscopically, membranes are essentially incompressible, so this limit is unphysical and we expect the layer contraction to evolve towards the isotropic patch calculation with increasing stress.

3 Application to Membranes in Flow

3.1 Physical Picture

We consider a Helfrich-stabilised lamellar phase with layer spacing d_0 (Fig. 3.1(A)). In flow, transverse membrane fluctuations are suppressed, leading to fewer collisions and hence more “space” between layers. If there is no permeation or other mechanism to change the layer number on the experimental time scale, the layer spacing remains fixed at its initial value (Fig. 3.1(B)). At sufficiently large

strains (Section 3.3.2) an instability will relieve the strain in favour of undulations via a non-equilibrium version of the Helfrich-Hurault effect. This then could be a precursor to either a stable modulated phase or an instability to onion formation. However, significant permeation due to passages, trans-membrane diffusion, or smectic defects, can lead to a layer spacing reduction after sufficient time for the required increase of layer number, as in Fig. 3.1(C). Which effect is seen depends on the rate of application of flow, the permeability and the defect structure, and the degree of crumpling.

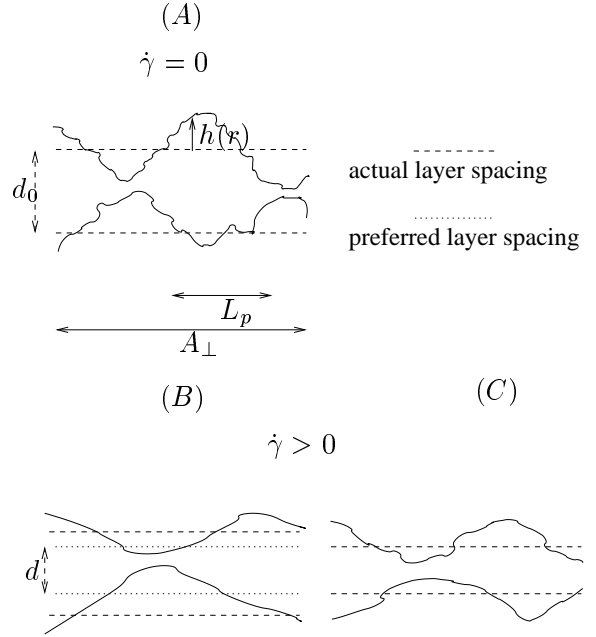


Fig. 3.1. Two different scenarios for a lamellar phase (A) subjected to flow. In (C) fluctuations are reduced and the layer spacing reduces due to the softened repulsive potential, while in (B) the equilibrium layer spacing is maintained because the system cannot relax (and form more layers).

3.2 Sources of Tension

Under the assumption that flow induces an effective tension in a lamellar phase, we apply the results of Section 2.2.1. This is heuristic, but we believe yields qualitatively useful results, as employed by Zilman and Granek [41]. Dynamically, tension corresponds to a tangential force resisting changes in total membrane area that induces a local normal force on the membrane. Hence, we contend that shear flow “irons out” small scale membrane wrinkles. Several dynamic effects can lead to an effective tension: (i) shear flow distorts and stretches membrane fluctuations, (ii) friction between the leaves of the bilayers increases the drag due to intra-bilayer dissipation in undulations, and (iii) intermembrane collisions induce a transverse membrane force. The first two effects are non-linear and yield

tensions that in the simplest case scales as $\dot{\gamma}^2$, while the latter effect is linear in $\dot{\gamma}$. All of these mechanisms are expected to be unimportant for flat, non-Helfrich membranes with weak equilibrium undulations.

The importance of convection and stretching can be estimated by balancing the restoring force on a wrinkle of wavenumber q with the viscous dissipation encountered in the flow in a thin film to find the typical undulation lifetime [40]. Fluctuations are influenced when the strain rate is of order the inverse lifetime of the slowest relevant undulations, which are those of wavelength the patch size L_p . This leads to an estimate for the critical strain rate $\dot{\gamma}_c$ at which undulations are appreciably suppressed by flow [40],

$$\dot{\gamma}_c \sim \frac{(k_B T)^{5/2}}{\eta d^3 \kappa^{3/2}} \quad (3.1)$$

where η is the solvent viscosity.

A more careful calculation begins with, for example, the Langevin equation for the affine convection of a fluctuating membrane** in the c orientation in a shear field $\mathbf{v} = \dot{\gamma} z \hat{\mathbf{x}}$,

$$\left[\partial_t + \dot{\gamma} h(\mathbf{r}, t) \frac{\partial}{\partial x} \right] h(\mathbf{r}, t) = -\kappa \int d^2 r' \Gamma(\mathbf{r} - \mathbf{r}') \nabla^4 h(\mathbf{r}', t) + \xi(\mathbf{r}, t). \quad (3.2)$$

The kinetic coefficient $\Gamma(\mathbf{r} - \mathbf{r}')$ depends on the details of the fluid-membrane coupling, with the form (in Fourier space) $\Gamma_{q\perp} \sim \eta^{-1} l^{\nu+1} q_{\perp}^{\nu}$. Here we give three examples of relaxation mechanisms that alter the exponent ν and the associated length scale l :

$$\Gamma_{q\perp} = \begin{cases} \eta^{-1} \zeta q_{\perp}^0 & \text{permeable} \\ \eta^{-1} q_{\perp}^{-1} & \text{isolated} \\ \eta^{-1} d^3 q_{\perp}^2 & \text{confined fluid/squeezing.} \end{cases} \quad (3.3)$$

The permeation length scale ζ depends on the size and the density of the pores and the membrane thickness***. For wavevectors $q_{\perp} \zeta \ll 1 \ll q_{\perp} L_p$ the membrane may be considered impermeable. In the confined fluid regime ($q_{\perp} d \gg 1$), squeezing of solvent within the confines of the surrounding membranes leads to $\nu = 2$ [61]. The case of $\nu = -1$ describes the hydrodynamic interaction of an isolated membrane in solvent ($q_{\perp} d \ll 1$) [62], with a length scale fixed by the wavevector. For permeable membranes, the characteristic length $\zeta < d$, with relevant wavevectors $q_{\perp} \epsilon \ll 1 \ll q_{\perp} \zeta$, where ϵ is some small length scale at which this dynamical description breaks down.

** In the dynamical description of the long wavelength variable $u(\mathbf{r})$ the convective term is $\dot{\gamma} z \partial_x u$, appropriate for wavelengths larger than the layer spacing and for fluctuation amplitudes u smaller than the layer spacing [27, 40].

*** A simple model of flow through circular pores of width w leads to $\zeta \sim t \psi^2 / w^4$, where ψ is the mean pore separation within the membranes.

The noise $\xi(\mathbf{r}, t)$ may or may not be related to $\Gamma(\mathbf{r} - \mathbf{r}')$ through the fluctuation-dissipation theorem, depending on the strength of the applied shear. Eq. (3.2) is a variation of an anisotropic Burger's equation with a convective non-linearity [63]. Upon coarse-graining Eq. (3.2) up to the collision length L_p , the convective non-linearity generates a dynamic response analogous to an effective scale-dependent tension,

$$\partial_t h_{\mathbf{q}\perp} + i \dot{\gamma} \sum_{\mathbf{k}\perp} (q_x - k_x) h_{\mathbf{k}\perp} h_{\mathbf{q}\perp - \mathbf{k}\perp} = - [\Gamma_{q\perp} \kappa q_{\perp}^4 + \Gamma_x(L_p, \mu) \dot{\gamma}^{\mu} q_x^2] h_{\mathbf{q}\perp}, \quad (3.4)$$

where $\Gamma_x(L_p, \mu)$ depends on the particular relaxation mechanism. Thus,

$$\sigma_{conv} \sim \frac{\Gamma_x(L_p, \mu)}{\Gamma_{q\perp}} \dot{\gamma}^{\mu}. \quad (3.5)$$

For example, for isolated membranes we find a “tension” of order

$$\sigma_{conv} \sim \frac{k_B T}{\kappa^2} L_p^5 \eta^2 \dot{\gamma}^2 q_{\perp}. \quad (3.6)$$

This calculation, along with results for the other relaxation mechanisms will be presented elsewhere [65]. A similar quadratic scaling was also estimated by Zilman and Granek [41], based on energetic arguments. It is important to recognize that, although the “tension” above applies, strictly, only to wavelengths of order the collision length, it is generated at all wavelengths larger than the smallest cutoff and grows during the coarse-graining procedure. We have chosen to model this tension, which is wavenumber-dependent, as an average value that applies for all wavenumbers. This certainly changes any quantitative predictions, but does not influence the qualitative aspects of our results.

Comparison of the bending and tension relaxation mechanisms of Eq. (3.4) leads to an estimate similar to Eq. (3.1) for the strain rate $\dot{\gamma}_c$ at which fluctuations are significantly suppressed

$$\dot{\gamma}_c \sim \frac{k_B T}{\eta d^3}. \quad (3.7)$$

If we consider a more detailed picture of the bilayers there are at least two more conceivable sources of tension. The two leaves of the bilayer exert transverse intermonolayer forces as they slide over each other. For flat membranes this simply renormalises the solvent viscosity; for highly crumpled membranes the viscosity is significantly enhanced,

$$\eta_{eff} \simeq \eta \left[1 + \frac{t \eta_b}{d \eta} \langle (\nabla_{\perp} h)^2 \rangle \right], \quad (3.8)$$

where η_b is the bulk viscosity of the bilayer material (typically alkyl tails). In this highly crumpled case there may also be an effective tension, or restoring force against the dissipation induced by bilayers with enhanced crumpling.

A third contribution comes from the tangential force incurred in interbilayer collisions. Because the bilayers retain their integrity they are moving at the velocity of the mean bilayer position, rather than at the velocity that would be determined by affine flow. The enhanced local shear rate near the collision event, over a length of order a bilayer thickness rather than the interlayer spacing, leads to an excess tangential force per unit length due to collisions, or equivalently a tension,

$$\sigma_{b-b} \sim \eta \frac{(d-t)}{t} \dot{\gamma} \frac{A_{con}}{L_p}. \quad (3.9)$$

Here, A_{con} is the collision contact area, expected to be quite small.

3.3 Scenarios in Flow

3.3.1 Layer Spacing Change

As mentioned in Section 2.2.1, an effective tension is expected to change the mean layer spacing in smectics with sufficient permeability. Specifically, either dislocation loops must be easily generated or the *lipid* permeability must be high enough for new layers to form before any incubation time for an instability or other transformation, such as to onions. Note that simple solvent permeability is not enough. Hence, we expect that highly defective membranes are most likely to exhibit a change in layer spacing under flow. An example of such a system is $C_{12}E_5$, which is known to be highly permeable in regions of the phase diagram [47] and dominated by the Helfrich interaction. In this case one expects a change in layer spacing governed by Eq. (2.17), with the tension σ given by a combination of collisions (Eq. 3.9) and convective effects (Eq. 3.6), schematically of the form

$$\sigma = \eta \dot{\gamma} [A + B \dot{\gamma}^{\mu-1}], \quad (3.10)$$

where A and B are poorly known.

Yamamoto and Tanaka found a flow-induced change of layer spacing in a $C_{12}E_5$ lamellar system only a few degrees away from the equilibrium lamellar-to-sponge transition. This does not, of course, necessarily validate our mechanism, since any mechanism that predicts the generation of new layers will be more susceptible in the presence of defects. In the vicinity of this temperature shear thinning behaviour was also observed, indicating that flow-induced change of structure was indeed occurring. They did not, unfortunately, report the quantitative dependence of layer spacing on strain rate, so it is difficult to make a precise comparison. Shear thinning has been seen in other layered systems (for example [22]) but as far as we know has not been correlated with a change of layer spacing.

The same $C_{12}E_5$ system has also been observed to form onions under shear in other regions of the phase diagram [66]. The dependence of structure formation on concentration, strain rate, shear history, and time would help to discern whether or not the mechanism we propose is

relevant for this system. Since flow modifies the fluctuation spectrum and the steric repulsion, the shape of the static structure factor should also change, which possibly explains the rounding of the Bragg peak observed by Yamamoto and Tanaka [36].

Note that, although defect generation is a necessary condition for changing the layer number, the presence of too many defects should invalidate layer suppression effects. For example, significant porosity at a scale less than the patch length implies a lack of integrity of the membrane. In this case, although on symmetry grounds the long wavelength theory would be the standard two fluid smectic hydrodynamics, the approximation of the microscopic membrane theory by a simple Helfrich Hamiltonian would break down. For example, we would not expect the theory to apply to the defect-ridden SDS/decanol/water lamellar system achieved by low concentrations of cosurfactant, that was observed to undergo transitions between a and c orientations [67]. In addition there have been suggestions that in some lyotropic lamellar systems the defect density of highly porous systems (before any discontinuous transition) can change continuously with the flow [47].

3.3.2 Instability

The alternative scenario is that in the absence of permeation, or if permeation is slow enough, the layer spacing cannot change from d_0 to d . Instead however, flow would induce an effective dilational strain γ , given by

$$\gamma = \frac{d_0 - d}{d}. \quad (3.11)$$

At sufficiently high flow, and hence strain, the system would become unstable to an analogue of the familiar Helfrich-Hurault effect, in which a smectic-A liquid crystal exchanges dilational energy for buckling energy for a large enough dilational strain. In that case, minimisation of the smectic elastic free energy determines the critical strain γ^* at the onset of the instability and the undulation wavevector q_\perp^* [29, 30].

The analogous effect for the sheared smectic is that fluctuations are suppressed by the flow, leading to a smaller “preferred” layer spacing; in the absence of layer-creation the effect is an induced strain, without actually applying a dilational pressure. We can gain a heuristic understanding of the effect by performing an equilibrium calculation for the critical strain, and compare it to the induced strain. The free energy of the smectic-A (Eq. 2.1) is adapted [30] to include the non-linearity required by rotational invariance[†], as well as a long wavelength symmetry breaking anisotropic tension arising from coarse graining the free energy (Eq. 2.12) up to the patch length, L_p :

$$F = \frac{1}{2} \int d^3r \left[\bar{B} \left[\partial_z u - \frac{1}{2} (\nabla_\perp u)^2 \right]^2 + K (\nabla_\perp^2 u)^2 + \frac{\sigma}{d} (\nabla_x u)^2 \right]. \quad (3.12)$$

[†] The correct form of Eq. (3.12) involves $\frac{1}{2} (\nabla u)^2$ rather than $\frac{1}{2} (\nabla_\perp u)^2$. This shifts γ^* and q^* by higher orders of λ/L .

In contrast to a positive tension acting on the ripples, imposing the constraints of fixed total and projected membrane areas, as in Ref. [41], leads to a negative tension (or lateral compression) that causes the membrane to buckle under sufficient shear (see Appendix A).

To calculate the stability, we consider a small perturbation δu around a strain induced displacement γ ,

$$u = \gamma z + \delta u \sin q_z z \cos q_x x \cos q_y y. \quad (3.13)$$

Upon linearising in δu , we find an undulatory instability with an undulation wavevector given by

$$q_x^* = 0, \quad q_y^* = \sqrt{\frac{\pi}{\lambda L}}, \quad q_z^* = \frac{\pi}{L}, \quad (3.14)$$

and a critical strain given by

$$\gamma^* \equiv \frac{d_0}{d^*} - 1 = \frac{2\lambda\pi}{L}, \quad (3.15)$$

where $\lambda = \sqrt{K/\bar{B}}$ is the penetration length and L is the sample thickness. If we ignore any renormalisation of \bar{B} due to the change in undulation spectrum, then the critical tension σ_c can be found, once γ^* is known, from Fig. 2.1. However, the suppression of fluctuations and the reduction in collisions diminishes \bar{B} (see Appendix B), which increases the critical strain and hence also increases the critical tension. An applied tension renormalised \bar{B} according to (Appendix B)

$$\begin{aligned} \bar{B} = & \frac{9\pi^2}{64} \frac{(k_B T)^2}{\kappa d^3} - \frac{k_B T \sigma}{4\pi\kappa d} \\ & - \frac{1}{16\pi^2} \left(\frac{5\pi}{4} - \frac{5}{\pi^2} - \frac{9}{16} \right) \frac{d}{\kappa} \sigma^2 + \dots \end{aligned} \quad (3.16)$$

If the strain is in the linear regime, as described by Eq. (2.17), assuming no permeation and $a \ll d_0 \ll L$ the effect on the reduction of \bar{B} is small and an instability is induced for large enough tension given by (from Eqs. 2.17, 3.11, 3.14, and 3.16)

$$\sigma > \sigma_c \simeq \frac{128\pi^2\kappa^2\phi}{tk_B TL} \left(1 - \frac{tk_B T}{4\pi\kappa\phi d_0} \right). \quad (3.17)$$

If $\phi = 0.2$, $k_B T = 4 \cdot 10^{-21}$ J, $t \sim 3$ nm, $L \sim 1$ mm and letting κ range from $0.2 - 4k_B T$ then σ_c is of the order $10^{-8} - 10^{-5}$ Jm $^{-2}$. In scaled parameters, this corresponds to $\hat{\sigma} \sim 10^{-3} - 10^{-1}$, and a very small critical strain is necessary, corresponding to the linear regime of Fig. 2.1. If $\sigma \sim \eta\dot{\gamma}d_0$ (owing to the difficulty of estimating the prefactors in Eq. 3.10) and $\eta \sim 1$ mPa-s then $\dot{\gamma}_c \sim 10^3 - 10^5$ s $^{-1}$ for same range of parameters. To achieve a value comparable with experiments, Zilman and Granek [41] rectified a similar discrepancy for the critical strain rate by replacing the solvent viscosity by the measured viscosity of the lamellar phase so that $\dot{\gamma}_c \sim 1$ s $^{-1}$ for low κ . On the other hand, reasonable experimental shear rates are obtained for small concentrations ($\phi \sim 0.01$). As in previous works [31, 16, 41, 32], we have taken L to be the system size. Another

possibility is that L corresponds to the lamellar grain size, whose scale is set by the defect density. In this case the reduction in \bar{B} and hence the change in critical strain and the strain rate will be significant.

The observation that the layer spacing does not change prior to onion formation does not seem to have been confirmed in experiment. However, the fact that most of the lamellar phases that undergo the onion transition seem to exhibit Newtonian or only weakly shear thinning flow (which is probably due to improvement in orientation of the layers or a reduction in defect density) indicates that flow is not bringing about such a structural change.

As might be expected, the membrane is most susceptible to undulations transverse to the applied flow direction. Hence, this instability is first to a stripe-like undulation, with stripes parallel to the flow direction, or equivalently with the wavevector in the vorticity direction. On the other hand, an isotropic tension that penalises Fourier modes in both directions favours square lattice buckling in preference to stripes. Although, as for an envisaged square lattice buckling, the mechanism from the stripe state to further transitions such as onions is unclear. Our result is consistent with recent work (unpublished) by Tanaka *et al.* that shows such an undulation in a $C_{12}E_5$ surfactant lamellar phase [66]. Similar behaviour has recently been demonstrated with simulations of a thermotropic lamellar phase [34]. The latter does not correspond to a Helfrich-stabilised lamellar system, while the experiments probably do. Recent experiments on $C_{10}E_5$ by Zipfel *et al.* revealed a kinetic intermediate between the *c*-oriented lamellar and onion phases, compatible with cylindrical multilamellar “leeks” [48]. Such leeks are compatible with an initial undulation in the layers, with wavevector parallel to the vorticity direction, that subsequently breaks the layers and stabilises in the cylindrical symmetry. We also note that the transient transitions to leeks and then onions occurred at roughly the same strain (or order a few thousand strain units), for different strain rates.

We emphasise that we have ignored Gaussian curvature, which is likely to influence transitions involving layer topology changes under shear. In equilibrium, reduction of salinity [10, 68] or temperature [69] or cosurfactant [70] are all known to decrease the Gaussian curvature modulus $\bar{\kappa}$, thus favouring phases consisting of spherical over bicontinuous structures. A $C_{10}E_3$ /water solution developed an onion transition upon reduction of the temperature at an imposed shear rate [49], which is consistent with the known decrease of $\bar{\kappa}$ with decreasing temperature in this system. Similarly, a low salt ionic surfactant AOT lamellar system showed no critical strain rate [10, 48], but rather onion formation at a characteristic critical applied strain with a time that increased dramatically for higher salt concentration and thus larger $\bar{\kappa}$. In this particular case, onion formation was independent of strain rate, suggesting a mechanism different from that we have proposed. Finally, at high enough concentrations of cosurfactant, the SDS/decanol/water system seemed to be prevented from forming onions [50], even though the system was less permeable. Here we suggest the increase in

Gaussian curvature may also be correlated with this observation.

4 Summary

We have studied the suppression of the undulations in a Helfrich-stabilised lyotropic lamellar phase in shear flow, by crudely modelling the flow as an effective anisotropic tension. This decreases the intermembrane compression modulus \bar{B} due to a reduction in fluctuations, and correspondingly changes the structure factor. There are two general consequences, depending on the permeability of the lamellar phase (under shear).

1. If permeation or defects allow the generation of new layers, such a system would eventually attain a new layer spacing, consistent with the flow-induced reduction of collisions.
2. If the system cannot change the number of layers, or the process is very slow, then either:
 - (a) The system can maintain the original layer spacing for low strain rates, with a concomitant effective strain due to the deviation from the preferred stable steady state.
 - (b) For higher strain rates, an instability to undulations along the vorticity direction can relieve the effective induced strain. A linear analysis does not allow us to determine whether or not such a state would result in a stable undulatory phase (as reported in simulations [34] and experiments [66]), become unstable to ripping layers to produce either cylinders with axes parallel to the velocity direction, as seen in a number of systems, or produce onions. In such a situation the layer spacing prior to forming the new state (striped undulation, cylinders, or onions) would not be expected to show a change in layer spacing.

Although the reduction of \bar{B} has a very small effect on the critical strain (or equivalently, the critical applied tension or strain rate) at which an undulatory instability may occur, the reduction in repulsion allows any attractive potential to become more significant. For highly swollen lamellar phases close to an equilibrium unbinding transition [59] there is the possibility of a flow-induced unbinding, which would probably be manifested in solvent expulsion or macroscopic phase separation.

In addition, we have discussed possible sources for the tension, including bilayer collisions, intra-bilayer dissipation and convection. The latter mechanism leads to a scale-dependent “tension” upon coarse-graining from the microscopic layer position $h(x, y)$ to the mean smectic layer displacement $u(x, y, z)$.

One implication of our result is that, in principle, lamellae and onions in flow are generally expected to have different layer spacings and hence different concentrations. Onions, particularly the large ones that appear at low shear rates and are the likely candidates for coexistence with lamellae [16], are very close in free energy and hence

layer spacing to the equilibrium lamellar phase, while the lamellae subject to shear flow could be subject to strong modification of their fluctuation spectrum. This would imply slow kinetics for the eventual transformation to onions, due to concentration changes, and non-trivial shapes for the measured flow curves, or ‘plateaus’, in regions of macroscopic coexistence [72].

Our work has focused on an instability to onion formation. We have not determined whether or not onions are metastable above a given strain rate, in which case the instability would be the analogue of an equilibrium spinodal. Indeed, it would be very interesting to study experimentally the history- and time-dependence upon cycling the strain rate or shear stress (both increasing and decreasing) through the lamellar-onion transition. Experiments on SDS/decanol/dodecane/water have indicated regions of concentration, or layer spacing and degree of crumpling, in which the transition is apparently continuous (low concentration or larger equilibrium layer spacing) and first order (high concentration and smaller layer spacing) [8, 7]. In addition, the history dependence may alter the eventual point of instability. For example, if the strain rate is increased slowly compared to the time scale associated with permeation, a reduction in layer spacing may be observed which would yield a higher critical strain rate. Further, if a system displays a shear induced reduction in layer spacing, onions might be formed if a strain rate larger than the critical strain rate is applied faster than permeation effects can occur.

We have assumed that flow acts as an effective tension. This is obviously quite crude, and forthcoming work will study the dynamics of individual membranes in flow. For membranes in the a -orientation, as studied by Ramaswamy to describe a layer collapse transition [24, 25], the convective term is linear, while in the c orientation, the convective term is non-linear, as in Eq. (3.2). On symmetry grounds, upon coarse-graining the fluctuations to a scale of order the patch size L_p between collisions, the convective non-linearity generates a tension-like restoring term in the long-wavelength dynamics, Eq. (3.4), which depends on the single membrane relaxation mechanism and is also, strictly, dependent on length scale and wavenumber in a very different form than a conventional “tension”.

We thank H Tanaka, T Kato, J Penfold, D Roux, AJ Bray, TCB McLeish, D Bonn, J Leng, and K Kremer for helpful discussions.

A Relation to Previous Work

In a related work, Zilman and Granek (ZG) [41], studied the effect of shear flow on the c -orientation of lamellar surfactant systems, to address the lamellar-to-onion transition. Our treatment differs from theirs in several respects. ZG advocate the physical picture that, for cylindrical Couette flow, layers retain their integrity so that the projected area is fixed by the experimental geometry. Shear flow removes small scale fluctuations and hence

would stretch the projected area of a free membrane. If this projected area is constrained, then the membrane can only undergo macroscopic buckling to redistribute undulations from small scale crumpling to larger scale undulations. Hence ZG model the coarse-grained membrane as experiencing a *negative* buckling tension. Our approach is quite different, and consists in examining the effect of a positive tension-like quantity on the underlying crumpling spectrum and hence the steady state layer spacing.

The ZG picture is certainly relevant if for example, most layers in a cylindrical Couette geometry have cylindrical topology with edges only at the cylinder ends. On the other hand, if most layers in the system do not encircle the centre Couette cylinder but end in edges, then they need not maintain a given projected area, but can adjust by moving defects. We feel that this relaxed constraint applies more generally than the fixed projected area constraint, but we acknowledge that line dislocation densities are notoriously difficult to determine experimentally.

Before outlining other differences we review the different layer variables for a lyotropic smectic:

$$h(x, y) = \begin{cases} \text{microscopic layer position} \\ (a < dx, dy < L) \end{cases} \quad (\text{A.1a})$$

$$u(x, y, z) = \begin{cases} \text{smectic layer displacement} \\ (L_p < dx, dy, dz < L), \end{cases} \quad (\text{A.1b})$$

where L is the system size, and dx, dy , and dz refer to differences of the independent variables x, y, z . The broken symmetry variable $u(x, y, z)$ describes the average layer displacement. In the undeformed state a layer is taken to be “flat”, $u(x, y, z) = 0$. In principle, $u(x, y, z)$ can be obtained by coarse-graining the highly crumpled microscopic variable $h(x, y)$ up to a length scale roughly of order the collision length L_p ; hence $u(x, y, z)$ is defined only on length scales larger than this cutoff. Conversely, $h(x, y)$ is defined down to a microscopic scale a , of order a surfactant head diameter. In performing the coarse-graining information about smaller length scales is retained, and resides in the other hydrodynamic variable, the concentration, which essentially measures the degree of crumpling at length scales smaller than the collision length L_p . Hence the free energy for lyotropic smectics is most naturally defined in terms of average layer displacement and concentration changes, although other combinations of these basic degrees of freedom are, of course, possible.

ZG draw an important distinction between different “projected areas”. ZG define the geometric area A_{geom} as the conventional projected area A_\perp imposed by sample geometry. For parallel plate rheometer A_\perp is the plate area, while for a Couette rheometer of cylinder height h , A_\perp is the cylindrical area $2\pi R h$ at a given radius R . ZG distinguish this area from a “physical” projected area A_{phys} , which can be interpreted as the area of the coarse-grained smectic variable u ; *i.e.* (in the Monge gauge)

$$A_{phys} = \int_{A_\perp} d^2r \left[1 + \frac{1}{2} (\nabla_\perp u)^2 \right]. \quad (\text{A.2})$$

This corresponds to the “constraint” introduced in Eq. (ZG-19), which is in fact not a constraint but a definition, as follows by examining their Figure 3 in conjunction with their discussion introducing physical projected area (A_o in their notation, in Figure 3 of their work).

By modifying the derivation of the Helfrich interaction ZG derive an expression for the macroscopic free energy $F_{ZG}[u, \Delta]$ (Eq. ZG-14a) of a lyotropic smectic as a function of the mean layer displacement variable $u(x, y, z)$ and the local change in physical projected area,

$$\Delta = \frac{\delta A_{phys}}{A_{phys}^{(0)}}. \quad (\text{A.3})$$

However, Δ cannot be an independent local hydrodynamic variable, like concentration (or volume fraction) in the standard two-fluid smectic description, because it is rigorously defined through Eq. (A.2) as a non-local function of $u(\mathbf{r})$. Hence, Δ does not contain, *a priori*, any information about small scale crumpling or concentration.

Although ZG claim that Δ may be eliminated in favour of the local volume fraction ϕ , and then “integrated out” to recover the free energy as a function of $u(\mathbf{r})$ at constant chemical potential, for which layer compressions are penalised by the usual modulus \bar{B} (ZG:Appendix B), this is not correct. The local volume fraction is defined by (Eqs. 2.10 and ZG-B.1)

$$\phi = \frac{tA}{dA_\perp}. \quad (\text{A.4})$$

ZG use this relation, at fixed membrane area A rather than fixed projected area A_\perp (Eq. ZG-B2), to relate changes in layer spacing, concentration, and A_\perp :

$$\frac{\delta\phi}{\phi} + \frac{\delta d}{d} = -\frac{\delta A_\perp}{A_\perp}. \quad (\text{A.5})$$

They assert that A_\perp may be taken to be the physical projected area A_{phys} and apply Eq. (A.3) to relate $\delta\phi$, δd and Δ , but this is inconsistent with the geometric definition above (Eqs. A.2 and ZG-19). They have already defined δd in terms of u , using the geometric relation (ZG-13)

$$\frac{\delta d}{d} = \frac{\partial u}{\partial z} - \frac{1}{2} (\nabla_\perp u)^2, \quad (\text{A.6})$$

correct to order θ^2 for small rotations θ . Combining Eqs. (A.2, A.5 and A.6) gives

$$\frac{\delta\phi}{\phi} = -\frac{\partial u}{\partial z}. \quad (\text{A.7})$$

Thus a small rigid body rotation[†] about the $\hat{\mathbf{y}}$ axis, $u \simeq -x\theta + \frac{1}{2}z\theta^2$ leads to the unphysical result $\delta\phi/\phi = -\frac{1}{2}\theta^2$.

Similarly, in the absence of the buckling tension σ (which they argue vanishes for zero shear) the final free energy ZG use (Eq. ZG-21a), obtained from Eq. (ZG-14a) by implementing the definition of physical area (Eq. A.2),

[†] In general, $u = -x \sin \theta + z(1 - \cos \theta)$.

is not invariant under small uniform rotations for $\sigma = 0$. ZG also consider a scenario in which the membrane area can vary at fixed layer number. In this case they minimise $F_{ZG}[u, \Delta]$ over Δ and use the resulting free energy to determine stability; however, this is inconsistent with the definition of Δ , according to Eq. (A.2).

A final problem concerns the non-linear analysis. The correct form of the rotational invariant term in the free energy (Eq. 3.12 and ZG-14a) involves $\frac{1}{2}(\nabla u)^2$ rather than $\frac{1}{2}(\nabla_\perp u)^2$. The effect of this approximation on the linear stability is negligible; the critical strain and wavevector shift by order λ/L where λ is the penetration length. However, a substantial correction is expected for a non-linear analysis of the buckled state, as in ZG-Section 4.2.

B Calculation of Tension-Renormalised Compression Modulus $\bar{B}(\sigma)$

To compute \bar{B} we follow the mean field variational approach of Rabin and Bruinsma [40], who calculated the free energy difference between a confined system and a corresponding set of free layers, and add an anisotropic tension. A related calculation has been performed by Lubensky *et al.* [73]. First, we replace the free energy of interacting membranes by an equivalent single membrane,

$$f = \frac{1}{2} \int d^2r \left[\kappa (\nabla_\perp^2 h)^2 + (\sigma + \mu) (\nabla_x h)^2 + \Gamma h^2 \right], \quad (\text{B.1})$$

where Γ and μ are variational parameters that maintain the equilibrium layer spacing, while σ penalises changes in excess area due to undulations in the x -direction. Assuming constant membrane thickness and area per molecule, μ is an effective chemical potential. For convenience, we consider a reservoir that admits material along the x direction and also penalises excess area. The last term is a harmonic potential that mimics membrane interactions, and thus determines the mean layer spacing.

The equilibrium distribution of membrane height fluctuations is given by

$$\rho_\perp(h) = \frac{\exp\left[-\frac{1}{2}\beta \sum_{\mathbf{q}_\perp} (\kappa q_\perp^4 + (\mu + \sigma) q_x^2 + \Gamma) |h_{\mathbf{q}_\perp}|^2\right]}{N}, \quad (\text{B.2})$$

where $\beta = 1/k_B T$ and

$$N = \int \prod_{\mathbf{q}_\perp} dh_{\mathbf{q}_\perp} \exp\left[-\frac{1}{2}\beta \sum_{\mathbf{q}_\perp} (\kappa q_\perp^4 + (\mu + \sigma) q_x^2 + \Gamma) |h_{\mathbf{q}_\perp}|^2\right]. \quad (\text{B.3})$$

By the equipartition theorem the mean layer fluctuations are

$$\langle h^2(\mathbf{r}) \rangle = \frac{k_B T}{4\pi^2} \int \frac{d^2 \mathbf{q}_\perp}{\kappa q_\perp^4 + (\mu + \sigma) q_x^2 + \Gamma}. \quad (\text{B.4})$$

The relation of $\langle h^2 \rangle$ to layer spacing (Eq. 2.6) determines Γ as a function of μ , while μ is finally determined by minimising the mean membrane free energy, given by (using Eq. B.2)

$$F = \langle f \rangle + k_B T \langle \ln \rho_\perp \rangle. \quad (\text{B.5a})$$

$$= \sum_{\mathbf{q}_\perp} \left[\frac{1}{2} (\kappa q_\perp^4 + \sigma q_x^2) \langle |h_{\mathbf{q}_\perp}|^2 \rangle + k_B T \left\langle \ln \left(\frac{\exp\left[-\frac{1}{2}\beta (\kappa q_\perp^4 + (\mu + \sigma) q_x^2 + \Gamma) |h_{\mathbf{q}_\perp}|^2\right]}{N} \right) \right\rangle \right]. \quad (\text{B.5b})$$

The free energy difference between free and confined membranes is

$$\Delta F = \frac{1}{2} k_B T \sum_{\mathbf{q}_\perp} \frac{-(\mu q_x^2 + \Gamma)}{\kappa q_\perp^4 + (\mu + \sigma) q_x^2 + \Gamma} + \ln \left[\frac{\kappa q_\perp^4 + (\mu + \sigma) q_x^2 + \Gamma}{\kappa q_\perp^4 + \sigma q_x^2} \right]. \quad (\text{B.6})$$

Expressing Γ to second order in $(\mu + \sigma)$,

$$\Gamma(\mu + \sigma) = \Gamma_0 + \Gamma'_0(\mu + \sigma) + \frac{1}{2} \Gamma''_0(\mu + \sigma)^2 + \dots, \quad (\text{B.7})$$

we find, using Eqs. (2.6, B.4),

$$\Gamma_0 = \frac{1}{\beta^2 \kappa (8\alpha d^2)^2}, \quad \Gamma'_0 = -\frac{1}{8\pi\alpha\beta^2 \kappa d^2}, \quad \Gamma''_0 = \frac{1}{\beta^2 \kappa} \left[\frac{3}{16} - \frac{27}{16\pi^2} \right]. \quad (\text{B.8})$$

For $\sigma = 0$, Γ_0 is the same while $\Gamma'_0 = -1/4\pi\alpha\beta^2\kappa d^2$ (correcting a sign error in [40]) and $\Gamma''_0 = (\frac{1}{2} - \frac{2}{\pi^2})\beta^2\kappa$. Substituting Eqs. (B.7) and (B.8) into Eq. (B.6) gives, after some calculation,

$$\frac{\Delta F}{A_\perp} = \frac{1}{128} \frac{1}{\kappa\beta^2\alpha d^2} + \frac{1}{8} \left(\frac{27}{16} - \frac{1}{\pi^2} \right) \frac{\alpha d^2}{\kappa} (\mu + \sigma)^2 + \frac{\sigma}{16\pi\beta\kappa} \left[\ln \frac{\sigma^2}{\kappa\Gamma} - 4 \ln 2 - \frac{5}{2} \pi^2 \alpha d^2 (\mu + \sigma) \right]. \quad (\text{B.9})$$

The compression modulus at constant chemical potential is given by

$$\bar{B} = d \left(\frac{\partial^2}{\partial d^2} \right) \left(\frac{\overline{\Delta F}}{A_\perp} \right), \quad (\text{B.10})$$

where $\overline{\Delta F}$ is the minimum free energy with respect to the chemical potential, yielding

$$\bar{B} = \frac{9\pi^2}{64} \frac{(k_B T)^2}{\kappa d^3} - \frac{k_B T \sigma}{4\pi\kappa d} - \frac{1}{16\pi^2} \left(\frac{5\pi}{4} - \frac{5}{\pi^2} - \frac{9}{16} \right) \frac{d}{\kappa} \sigma^2 + \dots \quad (\text{B.11})$$

As expected, Seifert's calculation of the potential between a membrane and vesicle in the presence of a small tension reduces to a similar result [58]

$$\bar{B} = \frac{9\pi^2}{64} \frac{(k_B T)^2}{\kappa d^3} - \frac{\pi k_B T \sigma}{32\kappa d} + \dots \quad (\text{B.12})$$

References

1. R. G. Larson, K. I. Winey, S. S. Patel, H. Watanabe, and R. Bruinsma, *Rheol. Acta.* **32**, 245 (1993).
2. G. H. Fredrickson, *J. Rheol.* **38**, 1045 (1994).
3. S. S. Patel, R. G. Larson, K. I. Winey, and H. Watanabe, *Macromolecules* **28**, 4313 (1995).
4. U. Wiesner, *Macromol. Chem. Phys.* **198**, 3319 (1997).
5. C. R. Safinya, E. B. Sirota, and R. J. Plano, *Phys. Rev. Lett.* **66**, 1986 (1991).
6. R. F. Bruinsma and C. R. Safinya, *Phys. Rev.* **E43**, 5377 (1991).
7. D. Roux, F. Nallet, and O. Diat, *Europhys. Lett.* **24**, 53 (1993).
8. O. Diat, D. Roux, and F. Nallet, *J. Phys. II (France)* **3**, 1427 (1993).
9. P. Panizza, A. Colin, C. Coulon, and D. Roux, *Eur. Phys. J. B* **4**, 65 (1998).
10. A. Leon, D. Bonn, J. Meunier, A. Al-Kahwaji, O. Greffier, and H. Kellay, *Phys. Rev. Lett.* **84**, 1335 (2000).
11. M. Bergmeier, H. Hoffmann, and C. Thunig, *J. Phys. Chem. B* **101**, 5767 (1997).
12. P. Sierro and D. Roux, *Phys. Rev. Lett.* **78**, 1496 (1997).
13. O. Diat, D. Roux, and F. Nallet, *Phys. Rev. E* **51**, 3296 (1995).
14. A. S. Wunenburger, A. Colin, J. Leng, A. Arneodo, and D. Roux, *Phys. Rev. Lett.* **86**, 1374 (2001).
15. P. Panizza, P. Archambault, and D. Roux, *J. Phys. II (France)* **5**, 303 (1995).
16. O. Diat, D. Roux, and F. Nallet, *J. Phys. II (France)* **3**, 1427 (1993).
17. G. Cristobal, J. Rouch, A. Colin, and P. Panizza, *Phys. Rev. E* **62**, 3871 (2000).
18. O. Dhez, F. Nallet, and O. Diat, *Europhys. Lett.* **55**, 821 (2001).
19. J. Zipfel, J. Berghausen, G. Schmidt, P. Lindner, P. Alexandridis, M. Tsianou, and W. Richtering, *PCCP Phys. Chem. Chem. Phys.* **1**, 3905 (1999).
20. J. Zipfel, P. Lindner, M. Tsianou, P. Alexandridis, and W. Richtering, *Langmuir* **15**, 2599 (1999).
21. M. E. Cates and S. T. Milner, *Phys. Rev. Lett.* **62**, 1856 (1989).
22. H. F. Mahjoub, K. M. McGrath, and M. Kleman, *Langmuir* **12**, 3131 (1996).
23. J. Yamamoto and H. Tanaka, *Phys. Rev. Lett.* **77**, 4390 (1996).
24. S. Ramaswamy, *Phys. Rev. Lett.* **69**, 112 (1992).
25. A. Al-Kahwaji and H. Kellay, *Phys. Rev. Lett.* **84**, 3073 (2000).
26. O. Diat and D. Roux, *J. Phys. II (France)* **3**, 9 (1993).
27. M. Goulian and S. T. Milner, *Phys. Rev. Lett.* **74**, 1775 (1995).
28. K. I. Winey, S. S. Patel, R. G. Larson, and H. Watanabe, *Macromolecules* **26**, 2542 (1993).
29. M. Delaye, R. Ribotta, and G. Durand, *Phys. Lett. A* **44**, 139 (1973).
30. P. G. de Gennes and J. Prost, *The Physics of Liquid Crystals*, 2nd ed. (Clarendon, Oxford, 1993).
31. P. Oswald and M. Kleman, *J. Phys (France) Lett.* **43**, L411 (1982).
32. A. S. Wunenburger, A. Colin, T. Colin, and D. Roux, *Eur. Phys. J. E* **2**, 277 (2000).
33. G. K. Auernhammer, H. R. Brand, and H. Pleiner, *Rheol. Acta* **39**, 215 (2000).
34. H. Guo, K. Kremer, and T. Soddemann, preprint.
35. W. Helfrich, *Z. Naturforsch.* **33a**, 305 (1978).
36. J. Yamamoto and H. Tanaka, *Phys. Rev. Lett.* **74**, 932 (1995).
37. F. Nallet, D. Roux, and S. T. Milner, *J. Phys (France)* **51**, 2333 (1990).
38. F. Nallet, D. Roux, C. Quiliet, P. Fabre, and S. T. Milner, *J. Phys. II (France)* **4**, 1477 (1994).
39. J. Prost, J. B. Manneville, and R. Bruinsma, *Eur. Phys. J. B* **1**, 465 (1998).
40. R. F. Bruinsma and Y. Rabin, *Phys. Rev.* **A45**, 994 (1992).
41. A. G. Zilman and R. Granek, *Eur. Phys. J. B* **11**, 593 (1999).
42. D. R. M. Williams and F. C. MacKintosh, *Macromolecules* **27**, 7677 (1994).
43. J. L. Harden and M. E. Cates, *Phys. Rev.* **E53**, 3782 (1996).
44. G. S. Grest, *Adv. Poly. Sci.* **138**, 149 (1999).
45. D. L. Polis, K. I. Winey, A. J. Ryan, and S. D. Smith, *Phys. Rev. Lett.* **83**, 2861 (1999).
46. J. A. Pople, I. W. Hamley, and G. P. Diakun, *Rev. Sci. Instrum.* **69**, 3015 (1998).
47. K. Minewaki, T. Kato, H. Yoshida, and M. Imai, *J. Therm. Anal.* **57**, 753 (1999).
48. J. Zipfel, F. Nettesheim, P. Lindner, T. D. Le, U. Olsson, and W. Richtering, *Europhys. Lett.* **53**, 335 (2001).
49. T. D. Le, U. Olsson, K. Mortensen, J. Zipfel, and W. Richtering, *Langmuir* **17**, 999 (2001).
50. J. Zipfel, J. Berghausen, P. Lindner, and W. Richtering, *J. Phys. Chem. B* **103**, 2841 (1999).
51. L. Golubovic and T. C. Lubensky, *Phys. Rev. B-Condens Matter* **39**, 12110 (1989).
52. M. Bachmann, H. Kleinert, and A. Pelster, *Phys. Rev. E* **6305**, 1709 (2001).
53. W. Janke, H. Kleinert, and M. Meinhardt, *Phys. Lett. B* **217**, 525 (1989).
54. D. Roux, F. Nallet, E. Freyssingeas, G. Porte, P. Bassereau, M. Skouri, and J. Marnigan, *Europhys. Lett.* **17**, 575 (1992).
55. D. Roux and C. R. Safinya, *J. Phys (France)* **49**, 307 (1988).
56. U. Seifert and S. A. Langer, *Biophysical Chemistry* **49**, 13 (1994).
57. U. Seifert and S. A. Langer, *Europhys. Lett.* **23**, 71 (1993).
58. U. Seifert, *Phys. Rev. Lett.* **74**, 5060 (1995).
59. S. T. Milner and D. Roux, *J. Phys. I (France)* **2**, 1741 (1992).
60. W. Helfrich and R.-M. Servuss, *Nuovo Cim.* **3D**, 137 (1984).
61. F. Brochard and J. F. Lennon, *J. Phys. (France)* **11**, 1035 (1975).
62. R. Messenger, P. Bassereau, and G. Porte, *J. Phys. (France)* **51**, 1329 (1990).
63. A. J. Bray, A. Cavagna, and R. D. M. Travasso, *Phys. Rev.* **E 64**, 012102 (2001).
64. A. J. Bray, A. Cavagna, and R. D. M. Travasso, *Phys. Rev.* **E 65**, 016104 (2001).
65. S. W. Marlow and P. D. Olmsted, (unpublished) (2002).
66. H. Tanaka, private communication.
67. J. Berghausen, J. Zipfel, P. Lindner, and W. Richtering, *Europhys. Lett.* **43**, 683 (1998).

- 68. H. N. W. Lekkerkerker, *Physica* **167A**, 384 (1990).
- 69. T. D. Le, U. Olsson, and K. Mortensen, *Physica B* **276**, 379 (2000).
- 70. G. Porte, J. Appell, P. Bassereau, and J. Marignan, *J. Phys. (France)* **50**, 1335 (1989).
- 71. M. Skouri, J. Marignan, J. Appell, and G. Porte, *J. Phys. II* **1**, 1121 (1991).
- 72. P. D. Olmsted, *Europhys. Lett.* **48**, 339 (1999).
- 73. T. C. Lubensky, J. Prost, and S. Ramaswamy, *J. Phys (France)* **51**, 933 (1990).